Atomic Electric Dipole Moment Measurement Using Spin Exchange Pumped Masers of ^{129}Xe and ^{3}He

M. A. Rosenberry* and T. E. Chupp
University of Michigan, Ann Arbor, Michigan 48109
(Received 1 August 2000)

We have measured the T-odd permanent electric dipole moment of ^{129}Xe with spin exchange pumped masers and a ^{3}He comagnetometer. The comagnetometer provides a direct measure of several systematic effects that may limit electric dipole moment sensitivity, and we have directly measured the effects of changes in leakage current that result when the applied electric field is changed. Our result, $d(^{129}\mathrm{Xe}) = 0.7 \pm 3.3(\mathrm{stat}) \pm 0.1(\mathrm{syst}) \times 10^{-27} e\,\mathrm{cm}$, is a fourfold improvement in sensitivity.

DOI: 10.1103/PhysRevLett.86.22 PACS numbers: 11.30.Er, 12.15.Ji, 32.10.Dk

The experimental study of CP and time reversal (T) invariance violation is over 40 years old. Remarkably, CP violation remains one of the most important open issues in elementary particle physics. The standard model allows CP violation via complex flavor mixing amplitudes of the Cabibbo-Kobayashi-Maskawa (CKM) matrix and via θ_{QCD}, the vacuum expectation value of the gluon field. However, the standard model cannot account for CP violation in the manner necessary for cosmological generation of the observed baryon asymmetry at the electroweak scale [1]. Many extensions of the standard model that predict CP violating observables for which the contribution of the CKM phase is small are compatible with the observed baryon asymmetry. Accelerator measurements continue to probe the parameters of CP violation in flavor changing K decays and B decays, however, for flavor nonchanging interactions, the best probe of CP or T violation is measurement of the permanent electric dipole moment (EDM) of an atom or the neutron.

An atomic EDM is a separation of charge along the total angular momentum $\vec{J}$ of the atom, i.e., $\mathbf{d} = g_d \mathbf{J}$. Because g_d changes sign under P and T, an EDM would arise from polarization of the atom by elementary particle interactions that violate T and, assuming CPT invariance, CP. For diamagnetic atoms, such as ^{129}Xe, an EDM would most likely arise due to CP violating interactions among the hadrons that induce a Schiff moment of the nucleus [2]. Sensitivity to this Schiff moment increases as Z^{2-3} due to the electron momenta, relativistic effects, and the size of the nucleus. Diamagnetic atoms are also sensitive to CP violating tensor neutral current interactions between the electrons and nucleus [3].

To measure an EDM, the energy splitting among the Zeeman sublevels is measured in the presence of parallel or antiparallel electric and magnetic fields. For a two state system, such as ^{129}Xe or ^{3}He, the Zeeman splitting is $\hbar\omega = 2\mu \cdot \mathbf{B} + 2\mathbf{d} \cdot \mathbf{E}$, which changes by $4\mathbf{d} \cdot \mathbf{E}$ when $\mathbf{E}$ is reversed with respect to $\mathbf{B}$, provided that $\mathbf{B}$ remains constant. In practice, $\mathbf{B}$ is never perfectly constant, in fact leakage currents contribute to $\mathbf{B}$ and may change when $\mathbf{E}$ is reversed. Therefore, any EDM experiment must also measure the magnetic field. In some measurements, the reported systematic error has been based on direct measurement of the leakage current and assumptions about its path. A comagnetometer, which measures the magnetic field in the same volume as the EDM sensitive species, can directly measure the effects of leakage current. The recently reported neutron EDM measurement used a ^{199}Hg comagnetometer [4], and other groups are incorporating comagnetometers into their experiments.

The most precise previously reported measurement of the ^{129}Xe EDM is $d(^{129}\mathrm{Xe}) = (0.2 \pm 1.1) \times 10^{-26} e\,\mathrm{cm}$ [5], and the most precise reported atomic EDM measurement is $d(^{199}\mathrm{Hg}) = (4 \pm 3) \times 10^{-28}$ [6]. The result from ^{199}Hg has been used to set limits on θ_{QCD} and a variety of phenomenological CP violating couplings among hadrons that would give rise to the Schiff moment of the nucleus [7]. The possibility that enhancements of the Schiff moments of ^{199}Hg and ^{129}Xe are greater than assumed previously [8] makes EDM experiments with diamagnetic atoms even more important.

Our approach, based on utilizing two species in the same volume, follows the work of Oteiza *et al.*, in which free induction decay (FID) of laser polarized ^{129}Xe and ^{3}He was used [9]. That result, $d(^{129}\mathrm{Xe}) = (1.5 \pm 10.1) \times 10^{-26} e\,\mathrm{cm}$ was limited by drifts associated with the changing magnetization during the FID [10]. In the current experiment, the stable oscillations of spin exchange pumped masers [11,12] of ^{3}He ($Z = 2$) and ^{129}Xe ($Z = 54$) greatly reduce the changes of magnetization so that the two masers act as nearly independent oscillators.

The apparatus is shown in Fig. 1. Many features and principles of operation are described in [11,12]. The central component is a bottle containing the ^{129}Xe and ^{3}He that is separated into a spherical pump cell and a cylindrical maser cell connected by a "transfer tube." The cell is made of borosilicate glass (Corning 7056 and 7052) with molybdenum electrode end plates on the maser cell. The end plates are attached with epoxy (Epo-Tek #353ND). The pump cell OD is 1.9 cm, the transfer tube 4 cm long with 0.4 cm ID, and the maser cell is 2 cm long with 1.27 cm ID. The glass portions of the cell are cleaned and

 0031-9007/01/86(1)/22(4)$15.00

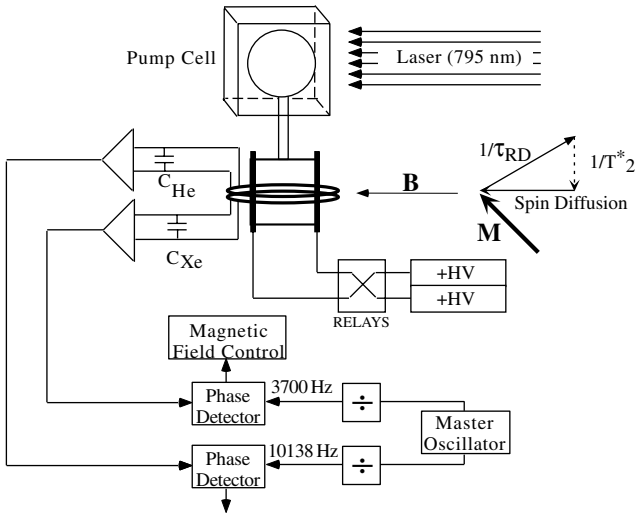

FIG. 1. Schematic of the EDM apparatus and magnetic field control. The ^{3}He maser oscillation is monitored with a circuit similar to the ^{129}Xe maser. The inset shows the Bloch vector **M** and the three torques that balance to sustain stable maser oscillations in the rotating frame.

coated with octadecyltrichlorosilane $[CH_3(CH_2)_{17}SiCl_3]$ [10,13,14], which reduces the ^{129}Xe spin relaxation rate due to wall interactions. The cells are evacuated on a UHV system and baked out for several days to a base pressure below 10^{-8} torr. Several milligrams of rubidium are distilled into the cells, and xenon gas (90% ^{129}Xe enrichment) is frozen into a cell held at 77 °K before N_2 and ^{3}He are added. The cell is then sealed with a torch. A typical sealed cell has the following partial pressures at room temperature: 110 torr xenon, 1115 torr ^{3}He, and 80 torr N_2.

Both ^{129}Xe and ^{3}He are polarized by spin exchange with laser polarized rubidium in the pump cell. At 120 °C, the saturated vapor density of rubidium is 2×10^{13} cm^{-3}, providing sufficient spin exchange rates for both maser species. Temperatures in the pump and maser cells are controlled at 120 °C and 40 °C to 10 mK or better (peak to peak). A free–running 30W fiber coupled laser diode array (Coherent model FAP-I) is tuned to 794.7 nm, the rubidium D1 resonance. Free–running laser diode arrays are relatively well suited to this application [15]. The estimated rubidium polarization in the pump cell is 68%. The estimated maser cell polarizations are 23% and 0.8%, respectively, for ^{129}Xe and ^{3}He. An end-corrected, double-wound solenoid produces the 3.15 G magnetic field. The entire assembly and the magnet are surrounded by three layers of passive μ–metal magnetic shielding with axial and transverse shielding factors of 1740 and 140 000, respectively.

The spins in the pump cell and maser cell are diffusively coupled by the transfer tube. In the maser cell the precessing ensemble of spins of each species can be represented by a Bloch vector **M** [11], with spins joining and leaving the ensemble through the transfer tube and through relaxation. The current induced in the pickup coils produces a torque that changes the Bloch vector and affects the induced current, providing gain. A Bloch vector of fixed magnitude and projection along the z axis, i.e., steady state oscillation, is sustained above threshold due to the equilibrium of three torques: spin diffusion from the pump cell, coherence relaxation, and radiation damping, which depends on **M**. These are indicated in Fig. 1, inset. The threshold condition for steady state maser operation requires that the coherence time for the freely precessing ensemble (T_2^*) be greater than the radiation damping time (τ_{RD}) [11]. Radiation damping requires sufficient polarization and good coupling to the pickup coil circuit. T_2^* is limited by the gradients of the magnetic field, wall relaxation, and spin diffusion out of the maser cell. Magnetic field gradients are controlled by variable end corrections on the solenoid and a set of coils designed to adjust gradients of the z components of **B** [10]. The electric field is produced by biasing the two electrodes of the cell with opposite voltages provided by two computer controlled power supplies (Glassman MJ30). A pair of high–voltage relays is used to reverse the connections, and power supply noise is low-pass filtered.

The pickup coil signals (10 and 2 μV for ^{129}Xe and ^{3}He, respectively) are amplified and then beat against reference clocks set about 25 mHz below each maser frequency. The phases of the beats are measured by two-phase lock-in amplifiers. The ^{129}Xe maser is phase locked to a separate reference oscillator by a PI control loop that corrects the solenoid current. Any change in the ^{129}Xe frequency, including that due to $\mathbf{d} \cdot \mathbf{E}$, will lead to a change of the solenoid current and a change of the ^{3}He frequency 2.8 times greater than the ^{129}Xe frequency change.

Data are acquired in 1000 or 2000 sec scans with constant electric field $\mathbf{E} = 0$ or ± 3.6 kV/cm. Between scans, the electric field is changed, a process that takes several minutes. Most data were taken using the sequence $(\ldots + - + - 0 - + - + 0 + - + - \ldots)$, though several runs had a different proportion of $\mathbf{E} = 0$ scans. Each set of 20 to 72 scans is a "run" and a separate EDM measurement. The magnetic field orientation was also reversed every 30–40 runs. This required retuning the magnetic field gradients and restarting the masers. Therefore each magnetic field reversal provides significantly different running conditions. All the data were taken with a single cell, and the orientation of the cell with respect to the room was not changed, though the cell orientation with respect to **B** did flip when the magnetic field was reversed.

We monitor a number of system parameters that might affect the maser frequencies. These include the temperature of the pump chamber, maser chamber, and tuning capacitors, the laser power, and leakage current. The helium beat frequency for each scan (with **E** fixed) is determined from a fit of the phase to a function linear in time and the two maser amplitudes. (The two species are magnetically coupled through their respective magnetizations, and changes in the maser amplitudes produce phase shifts of the two species [10,12].) Corrections to the ^{3}He beat frequency are based on linear correlations with measured

parameters. We used three different criteria for removing correlations based on F-test probability greater than 70%, 90%, or 98%. The data show negligible dependence on the criterion, and we use 90% for the final result. Though the magnetic field is controlled by feedback of the ^{129}Xe frequency, the control loop is not perfect, and small variations of the ^{129}Xe frequency are compensated by correcting the ^{3}He beat frequency for each scan. Then the series of frequencies in each run was corrected for slow drifts, up to third order in time, and for correlations with any of the following parameters: the temperature of the tuning capacitors that set the pickup coil resonant frequencies, room temperature, maser and pump cell temperatures, and laser intensity. Each of these parameters was determined to be uncorrelated with $\mathbf{E}$. Tuning capacitor temperature, which affects the maser coil circuit resonance frequencies leading to cavity pulling [16], was generally the only correction. The corrected ^{3}He frequency data for a single run are shown as a function of $\mathbf{E}$ in Fig. 2. The solid and dashed lines indicate the best fit dependence on $\mathbf{E}$ and $\mathbf{E}^2$, respectively, for the run. Note that the spread of ^{3}He frequencies is less when $\mathbf{E} = 0$, indicating that the high voltage induces noise in the pickup coils, probably through corona discharge and residual power supply noise. The EDM for a run is extracted assuming each string of four consecutive scans is correlated so that $\omega_{i+n} - \omega_i = \frac{2d}{\hbar}(E_{i+n} - E_i) + n\Delta + n^2\Delta^2$, where $n = 1, 2, 3$ and $i = 1 \ldots N - 3$ for N scans in the run, ω_i is the corrected ^{3}He frequency for each scan, d is the EDM value for the run, and E_i is the electric field for each scan [6,14]. The statistical error for each run is determined from the variance for the run. The dependence of the ^{3}He maser frequency on $\mathbf{E}^2$ is also extracted for each run.

A variety of systematic effects were considered and separately measured. The most important systematic effect is the leakage current that generates a magnetic field and frequency shift that cannot be distinguished from an EDM. Other changes in the apparatus and electronics correlated with the change of $\mathbf{E}$ could affect the reference oscillators, the control loops including the magnetic field phase lock, or the magnetic shields. Effects on the control loops are a particular concern, because the increased noise in the maser oscillators with $\mathbf{E} \neq 0$ changes the offset (droop) of the PI loops, which have finite gain at our modulation frequency of 0.05 or 0.1 milliHz. Other effects that depend on $\mathbf{E}^2$ include Stark shifts and the change of diamagnetic shielding of the nuclear magnetic moment, both of which are expected to be negligible.

The leakage current, monitored by measuring the change in ground current of the negative HV supply, varied. The largest changes, 20 pA, observed when the high voltage was reversed would produce a false EDM signal of $2 \times 10^{-27} e$ cm, assuming flow in a single turn around the maser cell. The role of the comagnetometer is to account for this effect. We directly measured the effect of applying a 1 μA current through a single turn of wire wrapped around the maser cell, confirming that a leakage current shift is rejected at a level below $10^{-28} e$ cm.

The frequency stability of the signal processing electronics was checked several times during the experiment in separate runs under normal conditions with maser cell high voltage but with signals derived from the reference oscillators substituted for the maser signals. Such effects were less than $10^{-28} e$ cm. Possible $\mathbf{E}^2$ effects, accounted for by correcting the data with the quadratic coefficient (see Fig. 2) combined with the high voltage reversal precision of 0 ± 10 V, were less than $10^{-28} e$ cm. It is possible that the magnetic shields are magnetized by the current from the high voltage supplies while charging the electrodes of the maser cell, which has a capacitance of $\approx$5 pf. The average charging current was less than 1 nA, but it flowed in a loop through the shields (a blunder). Shield magnetization would lead to a magnetic field control loop offset with memory of the change of $\mathbf{E}$ before a scan, and would appear in the $\mathbf{E} = 0$ scans. Analysis of the $\mathbf{E} = 0$ scans was statistically limited to $8 \times 10^{-27} e$ cm; however, such a charging effect would also appear as a systematic reversal of the EDM signal in the two orientations of $\mathbf{B}$. There is a 3.8σ difference of all data east compared to all data west, but it is not consistent with a reversal of the EDM signal.

The EDM measurement consists of 125 runs, each lasting between eight hours and several days. Improvements were made throughout the course of the experiment, and the later data are generally more precise. In Fig. 3, we

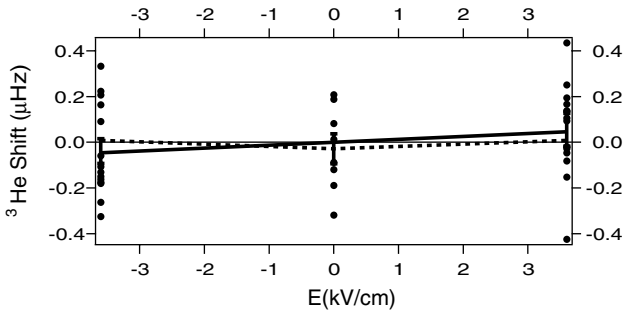

FIG. 2. Corrected ^{3}He beat frequencies for a single run plotted as a function of $\mathbf{E}$. The solid and dashed lines show the best fit dependence on $\mathbf{E}$ and $\mathbf{E}^2$, respectively.

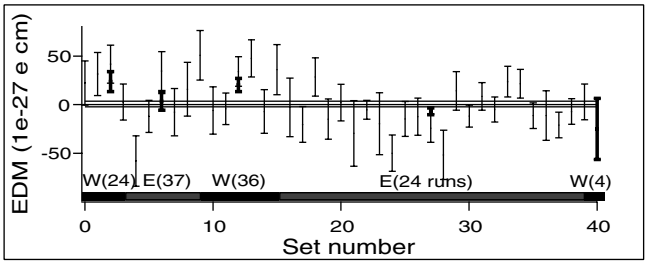

FIG. 3. EDM results for all data. Each point combines between one and eight consecutive runs so that each point has roughly equal statistical precision. Also shown as the heavy lines are the combined data, and the labels W(24) etc. indicate the direction of $\mathbf{B}$ and the number of runs between each flip of the magnetic field.

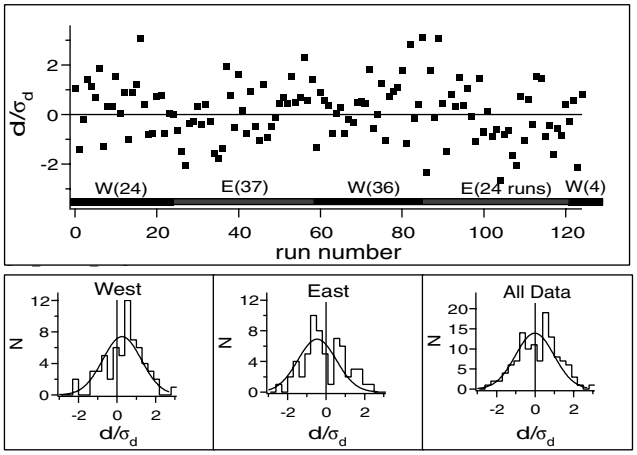

FIG. 4. Weighted EDM values ($\frac{d}{\sigma_d}$) for all runs displayed vs run number and as histograms.

show the EDM data combined into 40 separate consecutive periods with roughly equal statistical precision. Each period represents between one and eight individual runs. The direction of **B** is indicated. For all data west ($d_W = 19.8 \pm 5.7 \times 10^{-27} e$ cm) and for all data east ($d_E = -5.7 \pm 3.3 \times 10^{-27} e$ cm). When the data are further broken down they appear to fluctuate without a strong systematic dependence on **B**. We have further investigated the data by study of the weighted EDM values. In Fig. 4, we show d/σ_d for all runs and histograms for all data and for each orientation of **B**. The solid lines indicate normalized Gaussians with unit variance and best-fit centroids. We assume that the variations are random fluctuations so that we may therefore combine all runs in a weighted average, with the result $d(^{129}\mathrm{Xe}) = (+0.7 \pm 2.8) \times 10^{-27} e$ cm, with $\chi^2 = 168$ for 124 degrees of freedom. Our final result, $d(^{129}\mathrm{Xe}) = (+0.7 \pm 3.3) \times 10^{-27} e$ cm, is adjusted for $\chi^2_\nu = 1.35$. A positive $d(^{129}\mathrm{Xe})$ would be parallel to the nuclear angular momentum vector. The systematic errors discussed above have combined uncertainty less than $1 \times 10^{-28} e$ cm.

This ^{129}Xe EDM measurement is the most precise such result to date, and the use of the comagnetometer has provided a direct measurement of leakage current effects. Our result is 4× more sensitive than the ^{129}Xe EDM measurement of Vold [5], and only the ^{199}Hg experiment reports greater sensitivity to an EDM of any species [6]. The ^{199}Hg atomic EDM result is an order of magnitude more sensitive than our result, and is expected to have even greater sensitivity to CP violation due to the Z^2 dependence of the sensitivity of the atomic EDM to the nuclear Schiff moment. The nuclear theory of the Schiff moment is being reevaluated, and the sensitivity of ^{129}Xe and ^{199}Hg atomic EDMs to CP violation is expected to increase [8].

The potential for an improved measurement is indicated by the precision of the phase locked ^{129}Xe maser, about $0.5 \times 10^{-28} e$ cm for one day of running, reported in [11,12]. Phase locking corrects for any frequency shifts that would be measured by the free-running maser, and represents the ultimate precision of a measurement. The increased variance of the ^{3}He maser frequency with high voltage (Fig. 2) indicates that phase locking to the ^{129}Xe maser may be a major limitation. With separate magnetic field stabilization and technical improvements, we expect at least 1 order of magnitude improvement in sensitivity to $d(^{129}\mathrm{Xe})$ in a two species, comagnetometer experiment. Many of the techniques developed for this experiment are important for experiments with isotopes of radioactive radon that will be produced in large quantities at a rare ion accelerator (RIA). EDM measurements with radon are interesting due to the higher Z, possible laser based techniques, and the enhancements of the Schiff moment in octupole deformed isotopes [8,17].

Our collaboration with Rick Stoner, Ron Walsworth, and David Bear of the Harvard-Smithsonian Center for Astrophysics has been essential in advancing spin exchange pumped maser research. We also acknowledge the support of Erica Newman, Kevin Coulter, and Robert Welsh on aspects of this project. This work was supported, in part, by the National Science Foundation.

*Present address: Behlen Laboratory of Physics, University of Nebraska-Lincoln, Lincoln, NE 68588-0111.

[1] A. Riotto and M. Trodden, Annu. Rev. Nucl. Part. Sci. **49**, 35 (1999).
[2] L. I. Schiff, Phys. Rev. **132**, 2194 (1963).
[3] A. Martensson-Pendril, Phys. Rev. Lett. **54**, 1153 (1985).
[4] P. G. Harris *et al.,* Phys. Rev. Lett. **82**, 904 (1999).
[5] T. G. Vold, F. J. Raab, B. Heckel, and E. N. Fortson, Phys. Rev. Lett. **52**, 2229 (1984).
[6] J. P. Jacobs, W. M. Klipstein, S. K. Lamoreaux, B. R. Heckel, and E. N. Fortson, Phys. Rev. A **52**, 3521 (1995).
[7] V. M. Khatsymnovsky, I. B. Khriplovich, and A. S. Yelkhovsky, Ann. Phys. (N.Y.) **186**, 1 (1988).
[8] J. Engel, J. L. Friar, and A. C. Hayes, Phys. Rev. C **61**, 035502 (2000).
[9] E. R. Oteiza, R. J. Hoare, and T. E. Chupp, *Time Reversal: The Arthur Rich Memorial Symposium,* edited by M. Skalsey *et al.,* AIP Conf. Proc. No. 270 (AIP, New York, 1992).
[10] O. R. Oteiza, Ph.D. thesis, Harvard University, 1992.
[11] T. E. Chupp, R. J. Hoare, R. L. Walsworth, and B. Wu, Phys. Rev. Lett. **72**, 2363 (1994).
[12] R. E. Stoner, M. A. Rosenberry, J. T. Wright, T. E. Chupp, E. R. Oteiza, and R. L. Walsworth, Phys. Rev. Lett. **77**, 3971 (1996).
[13] M. S. Rosen, T. E. Chupp, S. D. Swanson, K. P. Coulter, and T. C. Welsh, Rev. Sci. Instrum. **70**, 1546 (1999).
[14] M. A. Rosenberry, Ph.D. thesis, University of Michigan, 2000.
[15] M. E. Wagshul and T. E. Chupp, Phys. Rev. A **40**, 4447 (1989); J. N. Zerger, M. J. Lim, K. P. Coulter, and T. E. Chupp, Appl. Phys. Lett. **76**, 1798 (2000).
[16] T. E. Chupp, E. R. Oteiza, J. M. Richardson, and T. R. White, Phys. Rev. A **38**, 3998 (1988).
[17] V. Spevak, N. Auerbach, and V. V. Flambaum, Phys. Rev. C **56**, 1357 (1997).